

Error budget in systems with time-dependent forcings

P. Sancho

Instituto Nacional de Meteorología, Centro Zonal de Castilla y León, Orión 1, 47071 Valladolid, Spain

Received: 20 May 1996 – Accepted: 10 December 1998

Abstract. The behaviour of the error growth is analyzed in several simple examples of systems with external time-dependent forcings. In some systems oscillations of the error around the saturation level can be observed. A common feature of these examples is the error growth dependence on initial time. In the examples here considered the improvement in the predictability derived from an adequate choice of the initial time is comparable to those obtained by reducing the initial errors.

case of the red-noise atmosphere with time-dependent terms the errors undergo, in the mean, an initial stage of exponential growth, but followed now by oscillations around the saturation level of the autonomous system.

A second conclusion derived from this study is the dependence of the error growth on the initial time t_0 (the time at which initial conditions are imposed). Error growth dependence on several factors have been clearly established in many studies. These factors are the initial error size (Trevisan, 1993), the weather regime and the location on the weather manifold (Keppenne and Nicolis, 1989). If the choice of the initial time modifies the analytical structure of the error growth, then t_0 can be viewed as a parameter playing an active role in predictability theory. In particular, the time necessary to reach the predictability limit will in general be different for different initial times (even supposing the size of the initial error similar in both cases). We show that in one of the models considered in this paper the improvement derived from an adequate choice of the initial time is comparable to those obtained by the reduction of the initial error size (the analysis error in operative weather forecasting models).

The plan of the paper is as follows. In Sect. 2 we study the impact of a time-dependent forcing in systems that obey the Lorenz law for error growth. In Sect. 3 the red-noise atmosphere with periodic forcing is analyzed. Finally, in the Discussion the main physical ideas involved in these models are considered.

1 Introduction

The general question of atmospheric predictability has gained increasing attention during the last years. The evolution of atmospheric flow is governed by nonlinear equations, whose solutions exhibit sensitive dependence on initial conditions. Some initial errors, large or small, will amplify and, after some time, render completely unreliable any forecast. Predictability is analyzed by the error budget that describes how fast forecast errors grow on average. A number of studies on error growth have been carried out using atmospheric models of varying complexity, from the simple analytical red-noise atmosphere (Fraedrich and Ziehmann-Schlumbohm, 1994) to simplified general circulation models or operational weather forecasting models (Schubert and Suarez, 1992; Lorenz 1982; Dalcher and Kalnay, 1987).

Atmospheric dynamics is an example of nonautonomous system with time-dependent external forcings. The incident radiation, driving the large scale motion of the atmosphere, is a periodic phenomenon. In climate dynamics the situation is even more compelling. The periodic variations of the orbital parameters seem to be one of the fundamental causes of climate change. We want to study the incidence of these time-dependent forcings in the theory of error growth. In particular, in this paper, we shall concentrate on some simple examples that can serve as a guide for more general studies. Despite the simplicity of the models we can obtain several interesting conclusions. The first one is the fact that some time-dependent systems do not obey the usual dynamics of the error growth, that is, an initial stage of exponential growth followed by saturation. We show that in the

2 Lorenz's law for error growth

The first attempt to deduce a law of error growth from real atmospheric data is found in the work of Lorenz (Lorenz, 1969). In the mean, the errors undergo an initial stage of exponential growth followed by saturation. As it turns out, this trend can be represented in a qualitative manner by a quadratic law, the logistic equation for the mean error X

$$\frac{dX}{dt} = A(X - X^2), \quad (1)$$

provided that the parameter A is suitably adjusted.

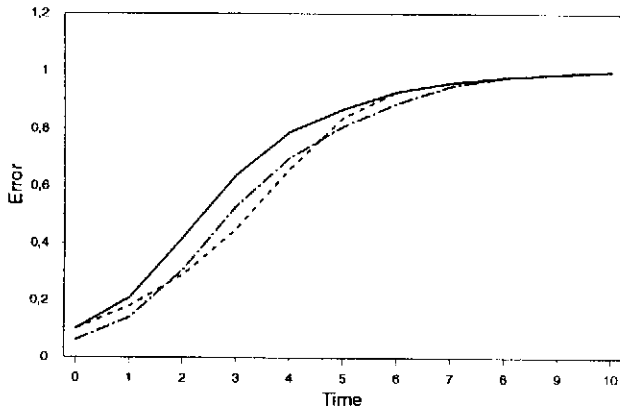


Fig. 1. Mean error X as a function of the dimensionless time $T = \omega t$. The solid, dashed and dash-dotted lines represent, respectively, the solutions of Eq. (7) for $X_0 = 0.1$ and $T_0 = 0$, $X_0 = 0.1$ and $T_0 = \pi$, and $X_0 = 0.066$ and $T_0 = 0$.

Let us consider an autonomous system

$$\frac{dx_j}{dt} = f_j(x_j), \quad (2)$$

whose mean error growth follows Lorenz's law. Equation (2) can represent, for example, the model used by Trevisan et al. with small initial errors (Trevisan et al., 1992).

Now, we introduce a periodic forcing in Eq. (2)

$$\frac{dx_j}{dt} = f_j(x_j) (1 + N \sin \omega t), \quad (3)$$

with N the amplitude and ω the frequency of the forcing.

Introducing the new variable $d\tau = (1 + N \sin \omega t) dt$, Eq. (3) reads

$$\frac{dx_j}{d\tau} = f_j(x_j). \quad (4)$$

Now the mean error will obey the equation

$$\frac{dX}{d\tau} = A(X - X^2), \quad (5)$$

equivalent to

$$\frac{dX}{dt} = A(1 + N \sin \omega t)(X - X^2). \quad (6)$$

The solution of Eq. (6) with initial condition $X(t_0) = X_0$ is

$$X(t) =$$

$$\left[1 + \left(\frac{1}{X_0} - 1 \right) \exp \left(-A(t - t_0) + \frac{NA}{\omega} (\cos \omega t - \cos \omega t_0) \right) \right]^{-1}. \quad (7)$$

Figure 1 shows this solution for two different values of the initial dimensionless time $T = \omega t$, $T_0 = 0$ and $T_0 = \pi$. The numerical values used for the constants are $A/\omega = 0.8$, $N = 0.25$ and $X_0 = 0.1$ (the initial error size is supposed to be equal in both cases). At a given intermediate time after imposition of initial conditions the two curves reach different values of error growth. The difference can be large, for instance, for $T = 3$ the values of the error are 0.65 and 0.45, and for $T = 4$ 0.79 and 0.66, respectively.

These differences imply different

Table 1. Predictability times derived from Eq. (8) for different values of the predictability limit (X^* from 0.2 to 0.8). The horizontal lines 1, 2 and 3 refer, respectively, to the initial conditions $X_0 = 0.1$ and $T_0 = 0$, $X_0 = 0.1$ and $T_0 = \pi$, and $X_0 = 0.066$ and $T_0 = 0$.

	0.2	0.3	0.4	0.5	0.6	0.7	0.8
1	0.9	1.4	1.9	2.3	2.8	3.3	4.0
2	1.2	2.0	2.4	2.8	3.4	4.2	4.8
3	1.3	1.8	2.7	3.2	3.7	4.0	4.8

predictability times. The predictability time t^* is defined as the time it takes for an initial error X_0 to reach a preassigned value X^* . This definition can be expressed in a mathematical form as

$$(X^*)^{-1} = 1 + \left(\frac{1}{X_0} - 1 \right) \exp \left(-At^* + \frac{NA}{\omega} (\cos \omega(t_0 B + t^*) - \cos \omega t_0) \right). \quad (8)$$

This equation cannot be solved analytically. In Table 1 we include the predictability times for different values of X^* . In all the cases the difference between both predictability times is important.

Finally, in order to compare the predictability improvements derived from the reduction of the initial error size and from the choice of the initial time, we include in Fig. 1 and Table 1 the error growth curve and predictability times for $T_0 = 0$ and initial error $2X_0/3$. We deduce from the curve that the error growth for $T_0 = \pi$ and X_0 is smaller for intermediate times. In particular, the predictability times for $X^* = 0.5$ are 2.8 and 3.2 (2.3 for $T_0 = 0$ and X_0), that is, improvements of 22% and 39%, respectively. From the predictability point of view a good choice of the initial time is comparable to a large (1/3) reduction of the initial error size.

3 Red-noise atmosphere

Time series observed in the atmosphere are characterized by some of the properties of red-noise processes. Because of this similarity the red-noise atmosphere has been used in many studies as a substitute of the real atmosphere. Recently Fraedrich and Ziehmann-Schlumbohm (Fraedrich and Ziehmann-Schlumbohm, 1994) have developed a predictability experiment in a red-noise atmosphere. By examining the lead-time-dependent error budgets of individual and ensemble forecasts, these authors derive analytically various measures of predictability. Despite the simplicity of the model, the error budgets share some qualitative features that may be compared to those of numerical weather-prediction and climate models.

In this paper we extend the model of these authors by including a temporal dependence in the red-noise process. The dynamics $Y_t = Y(t)$ consist of a deterministic part and an additive random part z_t

$$Y_n = Y_{n-1} f_{n-1} + z_n, \quad (9)$$

where

$$f_n = a + b \cos[\omega(n + n_0)], \quad (10)$$

and a and b are constants. n_0 indicates the time at which the process starts. The index n takes the values $0, 1, \dots$

The Gaussian white-noise z_n has zero mean $\langle z_n \rangle = 0$, variance $S_z^2 = \langle z_n^2 \rangle$ and vanishing crossed correlations $\langle z_n z_m \rangle = 0$ if n is different from m . We also suppose that Y_0 and z_i are statistically independent variables, $\langle z_i Y_0 \rangle = 0$. $\langle \rangle$ refers to the sample average.

Equation (9) can be expressed in terms of the initial condition Y_0 as

$$Y_n = Y_0 H_{0,n-1} + z_n + \sum_{i=1}^{n-1} z_i H_{i,n-1}, \quad (11)$$

where

$$H_{i,j} = f_i \cdot f_{i+1} \dots f_j, \quad (12)$$

is the product of the f 's between i and j .

3.1 Persistence forecasts

A first approach to the problem of predictability is provided by persistence forecasts. Persistence predicts the future states Y_n , using the initially given state Y_0 . The error budget of persistence forecasts is described by the evolution of the error variance $E_n = \langle (Y_n - Y_0)^2 \rangle$, where the sample average is taken over all the verification pairs. After simple statistical manipulations E_n becomes

$$E_n = A_n S_Y^2 + B_n S_z^2, \quad (13)$$

where $A_n = (1 - H_{0,n-1})^2$, $B_n = 1 + \sum_{i=1}^{n-1} H_{i,n-1}^2$ and $S_Y^2 = \langle (Y_0 - \langle Y_0 \rangle)^2 \rangle = \langle Y_0^2 \rangle$ is the initial variance of the variable Y (we suppose a zero mean $\langle Y_0 \rangle = 0$).

In Fig. 2 we represent Eq. (13) for two different values of the initial time n_0 , $n_0 = 0$ and $n_0 = \pi$. We have taken for a and b the values 0.9 and 0.4. The variances are $S_Y^2 = 0.6$ and $S_z^2 = 0.3$ and the frequency is $\omega = 0.85$. Moreover the third curve in the figure shows the same process with $b = 0$, that is, with no temporal dependence.

The three curves show an initial stage of exponential growth. The two time-dependent systems have important quantitative differences, for instance, we have for $n = 2$ $E_2(n_0 = 0) = 1.3$ and $E_2(n_0 = \pi) = 0.98$. These differences are also reflected into the predictability times. In systems with a discrete time variable the predictability time n^* is defined as the larger value of n for which the error is smaller than a preassigned predictability limit. For instance, taking the predictability limit as 1 we have $n^*(n_0 = 0) = 1$ and $n^*(n_0 = \pi) = 2$. In many studies the variance S_Y^2 serves as a predictability threshold and, consequently, is taken as the predictability limit. With this choice of the predictability limit we would have the same predictability times in both cases. The behaviour of autonomous and nonautonomous systems differs when the error of the autonomous process reaches the saturation level. At this stage, the systems with time dependent forcings show an oscillatory behaviour around a level close to the typical saturation level of the autonomous system. The two oscillations are similar, showing only a phase delay between the values of the two curves. This is a large value of the amplitude if we compare with the value of the saturation level 1.14. Moreover, the maximum and minimum values of the error at this stage are equal for both choices of the initial time, 1.41 and 0.97.

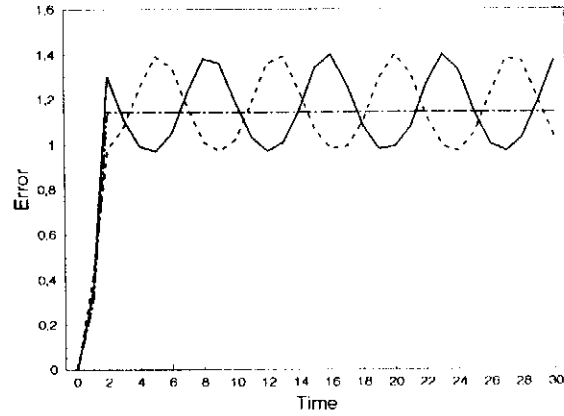


Fig. 2. Error growth E_n as a function of time n . The solid, dashed and dash-dotted lines represent, respectively Eq. (13) for $n_0 = 0$ and $n_0 = \pi$ (nonautonomous systems) and $b = 0$ (autonomous system).

3.2 Ensemble-mean forecasts

Now, we consider the error budget of ensemble-mean forecasts of a model with an external time dependent forcing. We denote by F_i an individual forecast by one member of the ensemble forecast ($i = 0, 1, \dots, M-1$). For a given field variable Y , the error budget is determined by the sample average of the squared forecast errors

$$\langle (Y_n - [F_i])^2 \rangle = \langle Y_n^2 \rangle + \langle [F_i]^2 \rangle - 2 \langle Y_n [F_i] \rangle. \quad (14)$$

The square brackets $[\]$ define the average over the lagged forecast ensemble:

$$[F_i] = \sum_{i=0}^{M-1} F_i / M. \quad (15)$$

To calculate the error budget we must introduce realizations of the individual forecasts F_i

$$F_i = Y_0 H_{0,i-1} + w_i + \sum_{j=1}^{i-1} w_j H_{j,i-1}. \quad (16)$$

The w 's are introduced to differentiate between noises in the verification (Y) and ensemble-forecast building mode (F_i). The initial condition (Y_0) is the same for both modes.

We study separately the three terms in the r. h. s. of Eq. (14).

1) $\langle Y_n^2 \rangle$. This is the simplest term and the calculation follows just the same steps of those done in the former subsection:

$$\langle Y_n^2 \rangle = S_Y^2 H_{0,n-1}^2 + S_z^2 (1 + \sum_{i=1}^{n-1} H_{i,n-1}^2). \quad (17)$$

Note that this formula is valid for $n \geq 1$. For $n = 1$ we have $H_{0,0} = f_0$ and $\langle Y_1^2 \rangle = S_Y^2 f_0^2 + S_z^2$.

2) $\langle [F]^2 \rangle$. This term can be written as

$$\langle [F]^2 \rangle = \frac{1}{M^2} \sum_{i=0}^{M-1} \langle F_i^2 \rangle + \frac{2}{M^2} \sum_{i=0}^{M-1} \sum_{j>i} \langle F_i F_j \rangle. \quad (18)$$

The term $\langle F_i^2 \rangle$ is given by an expression similar to Eq. (17) with obvious changes. On the other hand, $\langle F_i F_j \rangle$ ($j > i$) can be easily calculated

$$\langle F_i F_j \rangle = S_Y^2 H_{0,i-1} H_{0,j-1} + S_z^2 (1 - \delta_{i0}) H_{i,j-1} + S_z^2 \sum_{k=1}^{j-1} H_{k,i-1} H_{k,j-1}. \quad (19)$$

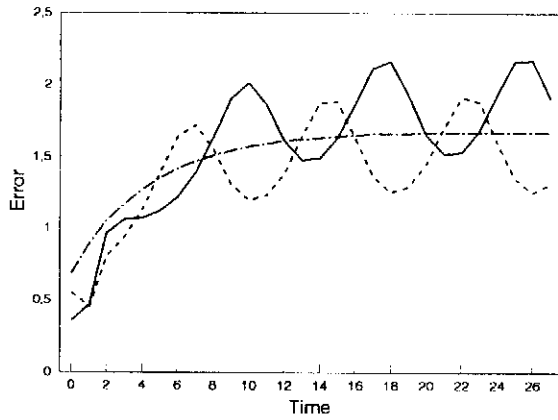


Fig. 3. Same as Fig. 2, but for Eq. (21).

δ is Kronecker's delta. Note that because the index k lies in the interval $(1, i-1)$ we have $\langle F_0 F_1 \rangle = S_T^2 f_0$, $\langle F_0 F_2 \rangle = S_T^2 f_0 f_1$, $\langle F_1 F_2 \rangle = S_T^2 f_1^2 + S_T^2 f_1 \dots$. We use the notation $H_{0,-1} = 1$.

3) $\langle Y_n[F] \rangle$. This term is also very simple and gives

$$\langle Y_n[F] \rangle = \frac{1}{M} S_T^2 H_{0,n-1} \sum_{i=0}^{n-1} H_{0,i-1}. \quad (20)$$

Putting together all these expressions and collecting separately the terms in the two variances we can calculate the error budget

$$E_n = A_n^* S_T^2 + B_n^* S_s^2, \quad (21)$$

where

$$A_n^* = H_{0,n-1}^2 + \frac{1}{M^2} \sum_{i=0}^{n-1} H_{0,i-1}^2 + \quad (22)$$

$$\frac{2}{M^2} \sum_{i=0}^{n-1} \sum_{j>i} H_{0,i-1} H_{0,j-1} - \frac{2}{M^2} H_{0,n-1} \sum_{i=0}^{n-1} H_{0,i-1},$$

and

$$B_n^* = 1 + \frac{1}{M} + \sum_{i=1}^{n-1} H_{i,n-1}^2 + \frac{1}{M^2} \sum_{i=0}^{n-1} \sum_{j=1}^{i-1} H_{j,i-1}^2 + \frac{2}{M^2} \sum_{i=0}^{n-1} \sum_{j>i} (1 - \delta_{i0}) H_{i,j-1} + \frac{2}{M^2} \sum_{i=0}^{n-1} \sum_{j>i} \sum_{k=1}^{j-1} H_{k,i-1} H_{k,j-1}. \quad (23)$$

The error budget is shown in Fig. 3 for $a=0.8$, $b=0.15$ and ω . The variances are $S_T^2=1$ and $S_s^2=0.3$. The third curve represents the autonomous process, $b=0$. The analysis of this system follows closely these presented in the previous subsection for persistence forecasts. The following features can be deduced from the curves. We observe again an initial stage of exponential growth. Taking the variance S_T^2 as the predictability limit the predictability times are $n^*(n_0=0)=2$, $n^*(n_0=\pi)=3$ and $n^*(b=0)=2$. After this initial stage we observe again an oscillatory behaviour of the error in the nonautonomous system. An important difference emerges when one compares to the case of persistence forecasts. As remarked earlier, the oscillations in persistence forecasts have the same amplitude, and maximum and minimum values for both choices of the initial time. However, in ensemble-mean forecasts only the amplitude of the oscillations is equal, approximately 0.34. The oscillations lie now in different

intervals, $(2.2, 1.52)$ for $n_0=0$ and $(1.94, 1.26)$ for $n_0=\pi$. Taking into account that the saturation level for the autonomous system is 1.68 we have that the error curves of these systems are most of the time, respectively, above and below the saturation level.

4 Discussion

We have presented an analysis of the dynamics of error growth in nonautonomous systems. The analysis is restricted to some very simple examples. The study of systems with time-dependent forcings can be justified from, at least, two points of view. Firstly, because atmospheric and climate dynamics are examples of nonautonomous dynamics driven by external, periodic forcings. Secondly, from a purely error growth theory point of view, the time-dependent terms are also necessary. For instance, Nicolis has suggested (Nicolis, 1992), that the logistic-like models of error growth must be augmented by time-dependent forcings in order to reflect the coupling of the error dynamics with the structure of the phase space.

In spite of the simplicity of the models here considered, the results obtained can be viewed as a preliminary step in the study of error growth in nonautonomous systems. Two principal conclusions have been derived from these models:

1) In the initial stage of exponential growth the error dynamics is sensitive to the choice of the initial time. As the predictability limit is reached at this stage, the different quantitative behaviours for different initial times imply a dependence of the predictability time on the initial time. This result justifies the view of consider the initial time as an active parameter in error growth theory. This dependence of the error growth on initial time can be easily understood by taking into account the fact that at different initial times the external forcings are different. We are placed at different regions in the mathematical space of external perturbations, and the respective error dynamics are modified. Moreover, the numerical estimations of Sect. 2 show that in some cases the improvement of the predictability time obtained by an adequate choice of the initial time is comparable to those obtained by a large reduction of the initial error. As we shall discuss in the next point, the error dynamics at the second stage will also depend, in general, on the initial time.

2) Autonomous and nonautonomous systems undergo an initial stage of exponential growth. Therefore, in spite of some quantitative differences, the underlying dynamics must be equivalent in both cases and must be dominated by the autonomous terms. After this initial stage the behaviour of both types of systems is, also qualitatively, different. Instead of the saturation stage typical of autonomous systems we observe in some nonautonomous models an oscillatory behaviour. Note that the model considered in Sect. 2 does not show these oscillations. This behaviour can be easily understood taking into account the type of temporal forcing introduced. The temporal term multiplies the right hand side of the differential equation and, consequently, the equation can be factored. We can see the temporal term as a modification of the mathematical measure of the variable time. We cannot expect that this simple modification of the system can modify qualitatively the error

dynamics.

The oscillations exhibited by nonautonomous systems can be explained by the contribution of several terms to the error dynamics. The autonomous terms contribute to the dynamics stabilizing the error and constraining the error variation to a finite interval (instead of a saturation level). On the other hand, the nonautonomous terms introduce an oscillatory temporal dependence on the error growth. A parameterization of the error growth that reproduces its main properties at this stage is

$$E_n = ESL + A \cos(\Omega n + \phi), \quad (24)$$

where ESL is the effective saturation level, defined as the level around which the error oscillates. Ω , ϕ and A are the frequency, phase delay and amplitude of the oscillation.

For persistence forecasts and $n_0=0$ and $n_0=\pi$ Eq. (24) reads $1.19+0.22\cos(n/7+2.43)$ and $1.19+0.22\cos(n/7+2.86)$. The two following features are noted:

(a) The effective saturation level differs from the saturation level of the autonomous system. This difference reflects the coupling between the autonomous and nonautonomous terms in the error dynamics. This coupling is a consequence of the nonlinearity of the system.

(b) The phase delay depends on the initial time. This dependence can be viewed as a manifestation of the fact that the system reaches the second stage at different times as a function of the initial time.

The parameterizations of the error growth in ensemble-mean forecasts at this second stage for $n_0=0$ and $n_0=\pi$ are $1.86+0.34\cos(n/7+2.14)$ and $1.6+0.34\cos(n/7+1.57)$. Now, the effective saturation level differs for different initial times. This difference reflects that the coupling between autonomous and nonautonomous terms depends on the choice of the initial time. In the case of persistence forecasts, the forecast is always the same, Y_n , for any initial time; the coupling is independent of the initial time. On the other hand, in the case of ensemble-mean forecasts the members of the ensemble are, in general, different and the coupling can depend on the initial time.

The conclusions obtained with the simple models here presented must be tested with more complex and realistic systems. In particular, the amplitude of the error oscillations obtained in this paper are large because of the large ratio b/a (deterministic autonomous/nonautonomous terms) used. In realistic models we must expect smaller amplitudes. Also, we must study systems with several simultaneous periodic forcings, as it is the case in atmospheric and climate dynamics.

Acknowledgments. This work has been partially supported by the DGICYT of the Spanish Ministry of Education and Science under contract n PB96-0451.

References

- Dalcher, A. and Kalnay, E., Error growth and predictability in operational ECMWF forecasts, *Tellus*, 39A, 474-491, 1987.
- Fraedrich, K. and Ziehmann-Schlumbohm, C. Predictability experiments with persistence forecasts in a red-noise atmosphere, *Q. J. R. Meteorol. Soc.*, 120, 387-428, 1994.
- Keppenne, C. L. and Nicolis, C., Global properties and local structure of the weather

attractor over Western Europe, *J. Atmos. Sci.*, 46, 2356-2370, 1989.

- Lorenz, E. N., Deterministic nonperiodic flow, *J. Atmos. Sci.*, 20, 130-141, 1969.
- Lorenz, E. N., Atmospheric predictability experiments with a large numerical model, *Tellus*, 34, 505-513, 1982.
- Nicolis, C., Probabilistic aspects of error growth in atmospheric dynamics, *Q. J. R. Meteorol. Soc.*, 118, 553-568, 1992.
- Schubert, S. D. and Suarez, M. J., Persistence and predictability in a perfect model, *J. Atmos. Sci.*, 49, 256-269, 1992.
- Trevisan A., Malguzzi, P., and Fantini, M., A note on Lorenz's law for the growth of large and small errors in the atmosphere, *J. Atmos. Sci.*, 49, 713-719, 1992.
- Trevisan A., Impact of transient error growth on global average predictability measures, *J. Atmos. Sci.*, 50, 1016-1028, 1993.